Study of Optical Forces Induced by Graphene Plasmonic Resonators on Nanoparticles near Their ENZ Frequencies

Puspita Paul*, Peter Q. Liu

Department of Electrical Engineering, University at Buffalo, the State University of New York, Buffalo, New York 14260, USA *Email: puspitap@buffalo.edu

Abstract: We demonstrate that optical forces induced by graphene plasmonic resonators on nanoparticles of Lorentz model materials are significantly larger than forces on dielectric nanoparticles. Such optical forces also exhibit intriguing characteristics around the ENZ frequencies. © 2020 The Authors

1. Introduction

Optical trapping of nanoscale particles using various plasmonic structures has been extensively investigated to surpass the classical diffraction limit in the conventional optical trapping mechanism, and already attained effective trapping of nanoparticles (NPs) with dimensions below 10nm. However, metallic plasmonic structures operate in the visible and near-infrared regions, which correspond to relatively high photon energy that can damage sensitive samples. Another major limitation of metallic plasmonic structures is the lack of real-time tunability of optical properties [1]. As alternative solutions, different types of tunable plasmonic materials (e.g., graphene, doped semiconductors and metal oxides) have been demonstrated for developing tunable plasmonic tweezers in the mid-infrared to terahertz region. For example, electrically tunable graphene nanoribbon (GNR) plasmonic structures for stable trapping and controlled transportation of dielectric NPs have been demonstrated [2]. Here, we present a systematic investigation of the optical forces induced by GNR plasmonic resonators on NPs made of Lorentz model materials, with the Lorentz resonance frequencies close to the GNR plasmonic resonance. Our numerical analysis shows that the trapping efficiency can increase by up to 60% for the Lorentz model NPs compared to dielectric NPs of identical sizes. In addition, the optical forces exhibit intriguing and anomalous characteristics around the Lorentz model materials' epsilon-near-zero (ENZ) frequencies, which may be exploited to realize new applications.

2. Structure description and simulation method

The schematic of the investigated GNR plasmonic structure is illustrated in Fig. 1(a). The 80nm wide GNR is patterned on a dielectric substrate with refractive index 1.53. The GNR Fermi energy is set to 0.4eV which leads to a plasmonic resonance at ~31.9THz, and the carrier scattering rate in terms of energy is set to 1meV (corresponding to a scattering time of ~0.66 ps and a carrier mobility of ~16000 cm²/Vs). Graphene was modeled as a 2D surface with an optical conductivity expression based on the Kubo formula. A 3nm thick encapsulation layer of the same refractive index (1.53) is added to protect the GNR from outside environment. A spherical NP (60nm diameter) made of a Lorentz model material is located at d=10nm above the surface of the encapsulation layer. The parameters for the Lorentz model include the static permittivity (ϵ_{∞} =14), the high-frequency permittivity (ϵ_{∞} =10), the Lorentz linewidth (δ_0 =0.32THz), and the Lorentz resonance frequency (f_0) is considered a tuning parameter which ranges from 23.9THz to 34.7THz. The x-coordinate of the NP is varied, and the electromagnetic field distribution is simulated using the FDTD method, while the optical force on the NP is calculated based on the Maxwell stress tensor method, which also agrees very well with the result obtained based on the Lorentz force density method. For comparison, we have also considered a dielectric NP (60nm diameter) with refractive index 3.74 (ϵ ~ 14) as the reference. A moderate excitation source intensity of 1mW/ μ m² is assumed in the simulation.

3. Results

As shown in Fig. 1(b)-(c), the spectrum (i.e., dependence on excitation source frequency) of the optical force induced by the GNR plasmonic resonator on the NP exhibits a strong dependence on the Lorentz resonance frequency f_0 of the NP material. When $f_0 \approx 27$ THz, the real part of the NP's Lorentz model permittivity becomes approximately zero (i.e. ENZ) at the GNR plasmonic resonance (~31.9THz) as shown in the inset of Fig. 1(b). We can further clearly see that when f_0 is not in the vicinity of 27THz, the optical force tends to trap the NP to the GNR across the entire simulated spectral range, and the peaks of the optical force spectra are near the GNR plasmonic resonance frequency, which are expected and similar to those of the reference dielectric NP. Moreover, when f_0 is higher than 28THz, the optical force on the Lorentz model NP is significantly larger than that on the reference dielectric NP; whereas when f_0 is lower than 26THz, the optical force on the Lorentz model NP is significantly smaller than that on the reference dielectric NP.

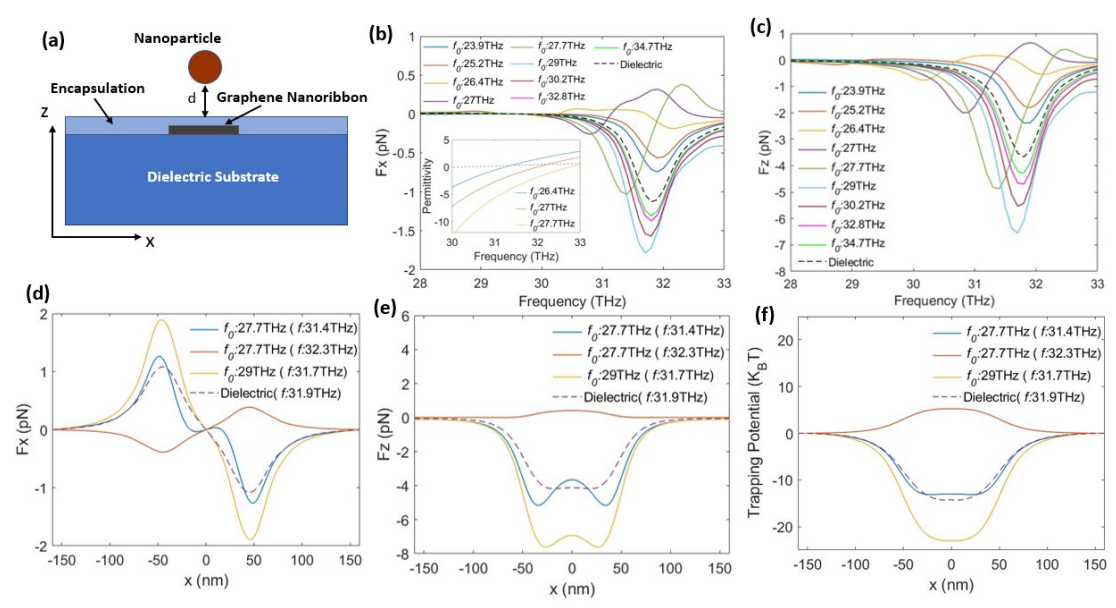


Figure 1 (a) Schematic of the investigated structure. (b) The x-component (Fx) and (c) the z-component (Fz) of the optical force as a function of the excitation source frequency (28-33THz), for various specified Lorentz resonance frequency values ranging from 23.9THz to 34.7THz. The NP is at a fixed x-coordinate, i.e. x=40nm (x=0 is the ribbon center). Inset of (c) shows the real part of the NP relative permittivity as a function of frequency for $f_0=27$ THz. (d) The x-component (Fx) and (e) the z-component (Fz) of the optical force, and (f) the corresponding trapping potential energy as functions of the NP's x-coordinate, for the specified excitation source frequencies f and NP Lorentz resonance frequencies f_0 . The calculated results of the reference dielectric NP are also plotted in (b)-(f) for comparison.

However, when f_0 is in the vicinity of 27THz (e.g. 26.4THz, 27THz and 27.7 THz in Fig. 1(a)-(b)) so that the real part of the NP's permittivity is near zero (i.e. ENZ) around the GNR plasmonic resonance, the optical force spectra exhibit drastically different line shapes. Specifically, both trapping and repulsive forces can be realized at different excitation frequencies, and the peak positions of the optical force spectra are no longer fixed to the GNR plasmonic resonance. Figure 1(d)-(f) show the calculated optical forces and the corresponding potential energy profiles as functions of the x-coordinate of the NP at the specified excitation source frequencies and assuming two Lorentz resonance frequencies (f_0 =27.7THz and 29THz, respectively). The results from the reference dielectric NP are also plotted for comparison. For f_0 =29THz, the optical force components tend to trap the NP and reach their peak values at $f \approx 31.7$ THz, while the corresponding trapping potential depth exceeds $20k_BT$ at room temperature, which is about 60% larger than that for the dielectric NP. For f_0 =27.7THz, the optical force has opposite signs in different spectral ranges. The trapping force components Fx and Fz reach their peak values at $f \approx 31.4$ THz, which correspond to a trapping potential depth larger than $10k_BT$ and comparable to that for the dielectric NP. The repulsive force components reach their peak values at $f \approx 32.3$ THz, which establish a potential barrier exceeding $5k_BT$. Such an ability to induce both trapping and repulsive forces can be exploited for various applications, e.g., sorting NPs with different Lorentz resonance frequencies.

4. Conclusion

In summary, we have systematically studied the optical force induced by GNR plasmonic resonators on NPs made of a material described by the Lorentz model. At the GNR resonance frequency, the optical trapping force and the corresponding potential energy depth for a Lorentz model NP can be significantly larger than those for a dielectric particle of identical geometry. On the other hand, when the GNR resonance lies within the ENZ frequency range of the Lorentz model NP, the optical force spectrum exhibits anomalous and intriguing characteristics, in that both trapping and repulsive forces can be realized at different excitation frequencies. Our study on the Lorentz model NPs can be applied to a broad range of materials, the permittivity of which may be determined by molecular vibrations, infrared-active optical phonons, intersubband transitions or interband transitions.

Acknowledgement

This work was partially supported by the National Science Foundation under the award number ECCS-1847203.

References

[1] M.L. Juan, M. Righini, R. Quidant, "Plasmon nano-optical tweezers," Nature Photonics 5, 349-356 (2011).

[2] P.Q. Liu, P. Paul, "Graphene Nanoribbon Plasmonic Conveyor Belt Network for Optical Trapping and Transportation of Nanoparticles," ACS Photonics 7, 3456-3466 (2020).